Modeling of Aluminum Nano-Particles Through Counterflow Combustion in Fuel-Lean Mixture

Mehdi Bidabadi[1], Yasna Pourmohammad[2], Moein Mohammadi[3], Hamed Khalili[4, *]

[1]Mechanical Engineering Faculty, Iran University of Science and Technology, Narmak, Tehran, Iran

[2]School of Mechanical Engineering, University of Kashan, Kashan, Iran

[3]Institute of Geophysics, Faculty of Physics, University of Warsaw, Warsaw, Poland

[4]School of Mechanical Engineering, Iran University of Science and Technology, Narmak, Tehran, Iran

Email address:
hamedkhalili19@yahoo.com (H. Khalili)
[*]Corresponding author

To cite this article:
Mehdi Bidabadi, Yasna Pourmohammad, Moein Mohammadi, Hamed Khalili. Modeling of Aluminum Nano-Particles Through Counterflow Combustion in Fuel-Lean Mixture. *International Journal of Fluid Mechanics & Thermal Sciences*. Vol. 3, No. 4, 2017, pp. 32-40. doi: 10.11648/j.ijfmts.20170304.11

Abstract: The combustion of aluminum nano-particles under fuel-lean conditions is studied in the counterflow configuration by means of analytical approach. The flame is assumed to consist of three zones: preheat, flame, and post flame regimes. By extraction and non-dimensionalizing of energy equations and then solving them in preheat zone and using perturbation method in the flame regime, analytical formulas for particles and gas temperature profile are presented. Then dimensionless ignition and ultimate flame temperatures, place of ignition point and flame thickness as a function of equivalence ratio in different strain rates are obtained. In addition, dimensionless ignition temperature, place of ignition point and flame thickness in terms of strain rate for different equivalence ratios are demonstrated. Reasonable agreement between the analytical solution of aluminum nano-particles counterflow combustion and experimental data is obtained in terms of flame temperature.

Keywords: Nano-Aluminum, Counterflow Combustion, Strain Rate, Flame Temperature

1. Introduction

Although the combustion of particles has been studied in many researches [20] [4] [25], the knowledge of metal nano-particles combustion needs to be improved and developed both in experimental and theoretical approach due to its importance in science and engineering specially in critical issues of fuel and energy and explosive hazards.

Combustion of aluminum particles is an important field of research, ignition and combustion of aluminum have been actively studied over the last five decades and a large body of experimental data was accumulated [2] [7] [8] [4] [10] [3]. Although aluminum particles have long been employed as a fuel ingredient in solid propellants, most previous work has been focused on micron or larger-size particles. Very limited effort [6] [16] [18] [23] was made to investigate the combustion of nano-sized aluminum particles.

In the early studies, Glassman recognized that metal combustion would be similar to droplet combustion, and therefore the D^2- law should be applied for burning time [1]. Many Researchers have done experiments to study the burning time and the ignition temperature of aluminum particle [11] [14] [23].

Dreizin and Trunov [11] burned aluminum droplets in air at room temperature and pressure of 1 atmosphere. Their reports showed a significant decrease in the aluminum burning time with the increase of the oxygen concentration. The conclusion of these observations was that, few would expect the exponent of D (particle diameter) to have the value of 2. A value of 1.5 to 1.8 was much more likely. To include the effect of different oxidizers, Brooks and Beckstead [7] suggested defining an effective mole fraction of oxidizer which includes the concentration of Oxygen, and Beckstead [1] suggested that with their coefficients proportional to 1, 0.22 and 0.6 respectively, the agreement between different studies is surprisingly consistent. In

another study, Shoshin and Dreizin [24] demonstrated that burning time of aluminum particles is a direct function of diameter.

Huang et al. [14] examined various parameters, such as the particle composition, equivalence ratio and particle size, on the burning behavior of bimodal aluminum particle/air mixtures in detail. They presented a model for burning time of aluminum nano-particles according to experimental results that have been used in the present work.

In another study, Huang et al. [15] theoretically investigated the combustion of aluminum particle dust in a laminar air flow. They explored a wide range of particle sized at nano and micron scales and obtained the flame speed and temperature distribution by numerically solving the energy equation in the flame zone. Furthermore, Huang et al. [13] studied the combustion of nano-sized aluminum particles with various oxidizers, including oxygen, air, and water in a well-characterized laminar particle laden flow by means of both numerical and theoretical approaches.

The research on combustion of aluminum nano-particles is critical in the design and optimization of combustor for underwater propulsion systems, since it will provide valuable information about particle injection and ignition, flame stabilization, and combustor heat transfer and thermal management [13]. The available literature shows that aluminum nano-particles can significantly improve the combustion properties of some energetic materials, especially for propulsion applications. Solid propellants containing aluminum nano-particles exhibit burning rates much higher (in some cases as much as 5 to 20 times higher) than the propellant formulations containing regular aluminum powder [17].

Aluminum nano-particles have gained importance because of their increased reactivity as compared with traditional micron-sized particle. Decreasing the size of aluminum particles increases their specific surface area, and hence decreases the burning time of the same mass of particles. Nevertheless, another consequence of decreasing the particle size is an increase of alumina mass fraction in the reactant powders passivated in air. All these features are important to practical applications.

Particle diameter is very important in determining the relevant combustion mechanisms. A large diameter particle at high pressure may burn under diffusion-controlled conditions, whereas a small particle at low pressure may burn under kinetically controlled conditions [28]. Heat conduction between micron-sized particles and the surrounding gas is in continuous regime but heat loss from a spherical nano-particle to surrounding gas is usually in transient regime [19] and they have a lower minimum burning energy, melting point, activation energy and reaction enthalpy.

From the fact that in many practical applications the flow field is appreciably strained, to yield realistic flame prediction under such conditions, counterflow configuration is suitable for studying these cases. Over the last few decades, the counterflow configuration has been extensively adopted in theoretical, experimental and numerical studies as a means to investigate various physical effects on real flames, such as stretch, preferential diffusion, radiation and chemical kinetics [9] [26] [27].

Although much useful information has been obtained from the preceding studies, the current knowledge about aluminum dust particles combustion is far from completion. In the present work, combustion of aluminum nano-particles for fuel-lean mixtures in a premixed counterflow configuration has been studied by means of analytical solution and the trend of dimensionless ignition and ultimate flame temperatures, place of ignition point and flame thickness with changes of equivalence ratio and strain rate have been demonstrated that expected results such as increasing ignition temperature with a rise in the value of particle concentration, confirm earlier experiments [14] [15].

2. Mathematical Modeling

2.1. Governing Equations

In the current analysis, we are primarily concerned with fuel-lean mixtures. The flame is assumed to consist of three zones: preheat, flame, and post flame regimes. In the preheat zone, the reaction rate is negligibly small, and the gas is heated by conduction from the flame zone. Particles are heated by the surrounding gas until their temperature reaches its ignition point. In the post flame zone, the combustion is completed. In the flame zone, particles are ignited and totally consumed. The particle-burning rate usually depends on the local particle radius, local oxidizer concentration, and the mass and thermal diffusivities of oxidizer. Because of the excess of the oxidizer in a fuel-lean mixture, the total particle burning time is assumed to be equal to the burning time of a single particle. Fundamental assumptions in this analysis are:

1. Aluminum Nano particles have uniform distribution in mixture.
2. The particle velocity is approximately equal to the gas velocity and it is variable along the path.
3. The gravitational effects and heat transfer by radiation are neglected.
4. In the preheat zone, the reaction rate is negligibly small.
5. Combustion of dual-fuel particle-laden flows was examined by Goroshin et al. [12] for aluminum-manganese dust mixtures. According to that, burning time is taken to be known, and the data is obtained from experimental results of Huang et al. [14].
6. Aluminum particles vaporize before combustion and react with air in gas phase.
7. Flow of fuel-lean mixture is assumed to be laminar.

In the current analysis, a one dimensional model with axial symmetry and premixed flame in counterflow configuration has been used. In Figure 1 the considered configuration includes planar twin flames. Reactants enter from $\pm x'$ direction and gases exit from $\pm z'$ direction. According to configuration's symmetry, all the calculations are done for $x' < 0$. In the following equations, subscripts 'f', 'u', 's', 'st' and 'i' denote the flame zone, the entrance situation, the solid

particle, the stoichiometric state and the start point of flame zone, respectively. Also 'E' and 'R' denote activation energy and universal gas constant.
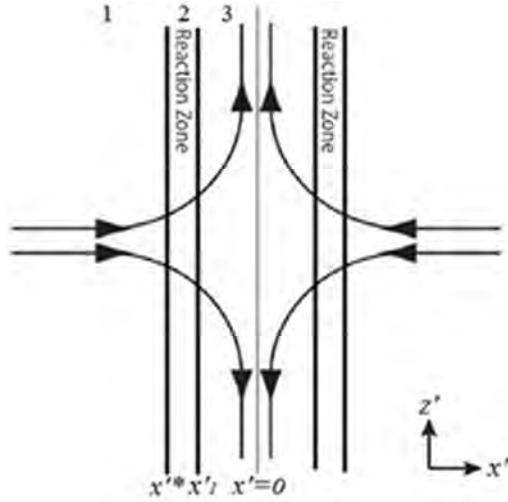

Figure 1. *Counterflow configuration and planar premixed twin flames.*

Velocity field is obtained by definition of strain rate Eq. (1) in Cartesian coordinate that 'a' represents strain rate, and as a function of 'x''.

$$2a = -\frac{1}{\rho}\frac{d(\rho v)}{dx'} \tag{1}$$

Since the density of aluminum particle varies during the reaction, the following formulation has been used to take into account the particle's density variation:

$$x = \int_0^x \frac{\rho}{\rho_u}dx' \tag{2}$$

So the governing equations are as follow:

$$-2\rho_u axc\frac{dT}{dx} = \lambda_u\frac{d^2T}{dx^2} + \omega_f\frac{\rho_u}{\rho}Q \tag{3}$$

$$-\frac{2}{3}\rho_s c_s ax\frac{dT_s}{dx} = \frac{\lambda}{r^2}(T - T_s) \tag{4}$$

Equations (3) and (4) are the energy conservation equations for gas and solid particles, respectively. In the Eq. (3), c represents specific heat of gas, λ_u defines heat conduction coefficient, Q shows heat of reaction per unit mass and ω_f is reaction rate in flame zone that according to the work of Huang et al. (Huang et al., 2007), has been obtained from the following equation:

$$\omega_f = \frac{\sigma}{\tau_b} \tag{5}$$

Where σ represents concentration of particle and τ_b represents burning time, obtained from the following experimental formution, by assuming that the width of reaction zone is short:

$$\tau_b = \frac{d^{0.3}}{c_2 X_{eff}}e^{(\frac{E}{RT_f})} \tag{6}$$

Where d and X_{eff} represent the particle diameter in 'cm' and effective mole fraction of oxidizer that has been obtained by Eq. (7), respectively. The Constant parameter c_2 is equal to 5.5×10^4.

$$X_{eff} = C_{O_2} + 0.6C_{H_2O} + 0.22C_{CO_2} \tag{7}$$

2.2. Analytical Solution

The non-dimensional parameters are introduced as fallows

$$\theta = \frac{T}{T_u}, \theta_s = \frac{T_s}{T_u} \tag{8}$$

$$y = x\sqrt{\frac{\rho_u c}{\lambda_u a\tau_b^2}} \tag{9}$$

$$\varphi = \frac{\sigma}{\sigma_{st}}, \kappa = a\tau_b \tag{10}$$

$$\mu = \frac{\sigma_{st}Q}{\rho C_p(T_{si} - T_u)} \tag{11}$$

$$\gamma = \frac{(6\times10^{-4})\lambda}{a\rho c_s(x_{eff}\tau_b c_2)^{\frac{20}{3}}}e^{(\frac{20E}{3RT})} \tag{12}$$

Substituting the above parameters into Eq. (3) and (4), we obtain the following non-dimensional equations:

$$2\kappa^2 y\frac{d\theta}{dy} = \frac{d^2\theta}{dy^2} + \mu.\varphi.\kappa(\theta_{si} - 1) \tag{13}$$

$$-y\frac{d\theta_s}{dy} = \gamma(\theta - \theta_s) \tag{14}$$

Boundary conditions in preheated zone are as follows:

$$\begin{aligned} y \to -\infty &: \theta = \theta_s = 1 \\ y \to y^{*-} &: \theta = \theta_i, \theta_s = \theta_{si} \end{aligned} \tag{15}$$

Where θ_i and y^* represent dimensionless ignition temperature and place of ignition point, respectively. In the preheated zone, the reaction is assumed to be negligible and therefore the solution of Eq. (13) for the gas temperature is as below:

$$\theta = (\theta_i - 1)\frac{erf(\kappa y) + 1}{erf(\kappa y^*) + 1} + 1 \tag{16}$$

By substituting that in Eq. (14), the solid nano-particles temperature is obtained from the following equation:

$$\theta_s = \frac{(\theta i - 1)}{1 + erf(\kappa y^*)}(1 + erf(\kappa y) + \frac{\kappa y(\kappa^2 y^2)^{\frac{\gamma-1}{2}}}{\sqrt{\pi}}\Gamma(\frac{1-\gamma}{2}, \kappa^2 y^2)) + 1 \tag{17}$$

In the present work, the method of perturbations is used to obtain the solution of the governing differential equation. Perturbation techniques [21] [22] are widely applied to obtain approximate solutions of these equations involving 'ε' as a small parameter. In the reaction zone from Eq. (13) and by means of Perturbation Method, dimensionless temperature of the gas is obtained as follows:

$$\varepsilon = \kappa^2 \tag{18}$$

$$\theta = \theta_0 + \varepsilon\theta_1 + \varepsilon^2\theta_2 + ... \tag{19}$$

$$\theta = -\frac{b}{2}y^2 + by_1y + \theta_1 - \frac{by_1^2}{2} + \varepsilon(\frac{b}{6}y^4 - \frac{b}{3}y_1y^3 + \frac{b}{3}y_1^3y + \theta_1 - \frac{b}{6}y_1^4)$$
$$+\varepsilon^2(\frac{-2b}{45}y^6 + \frac{b}{10}y_1y^5 - \frac{b}{9}y_1^3y^3 + \frac{b}{10}y_1^5y + \theta_1 - \frac{2b}{45}y_1^6) + O[\varepsilon^3] \tag{20}$$

$$b = \mu\varphi k(\theta_{si} - 1) \tag{21}$$

With Eq. (17) and (20) and additional boundary condition the problem can be solved. According to the work of Goroshin [12], burning time is assumed to be known and can be obtained from the Eq. (6). By this assumption and using τ_b, dimensionless place of flame ending point, y_1 and flame thickness, δ is obtained as below:

$$y_1 = y^* \exp(-\kappa) \tag{22}$$

$$\delta = y_1 - y^* \tag{23}$$

By using Eq. (17), (20), (22) and boundary conditions (15), we are able to find θ_i, θ_1 and y^* in any equivalence ratio.

3. Results and Discussion

In this section we present the results of analytical solution of the equations. According to the profiles obtained for the dimensionless temperature in preheated and flame zone, the following diagrams have been drawn. The trend of dimensionless ignition and ultimate flame temperatures with change of equivalence ratio in different strain rates can be seen in these diagrams.

According to Figure 2 and Figure 3, with a rise in the value of particles concentration, the ignition temperature increases. Also, the ignition temperature tends to decrease as the value of strain rate rises. Similarly, the same trend can be seen for ultimate flame temperature. It should be noted that there is little difference between the values of ignition and ultimate flame temperature and it is because of very small flame thickness. The obtained results from the presented model show reasonable agreement with the earlier data [13] For example, we expected increasing ignition temperature with a rise in the value of particle concentration, which Figure 2 confirms this idea.
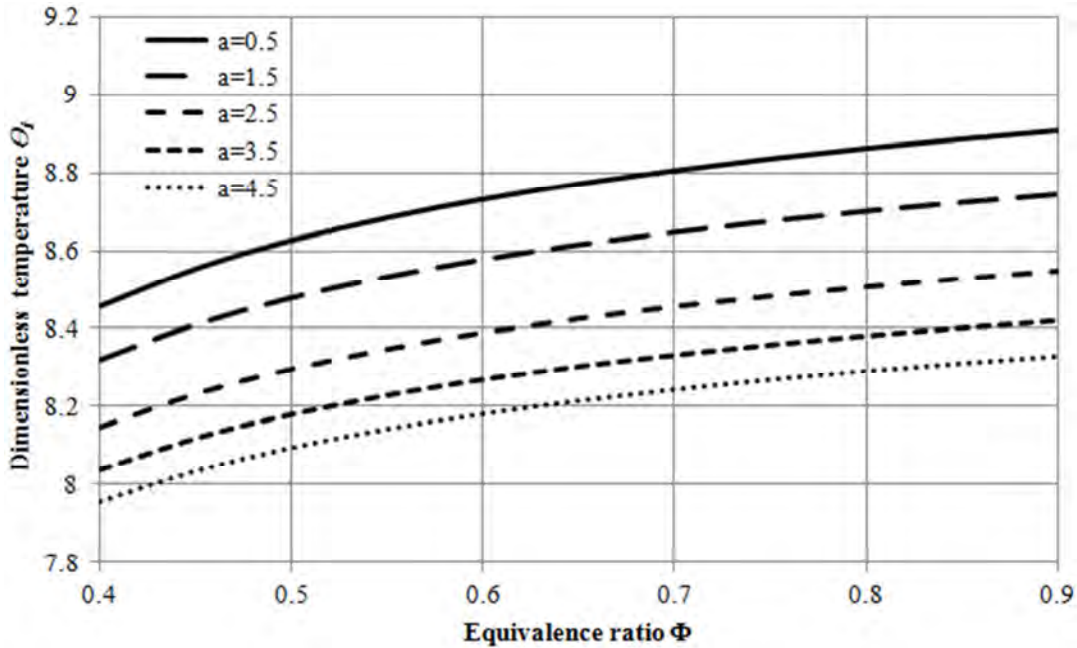

Figure 2. Dimensionless ignition temperature as a function of equivalence ratio in different strain rates.
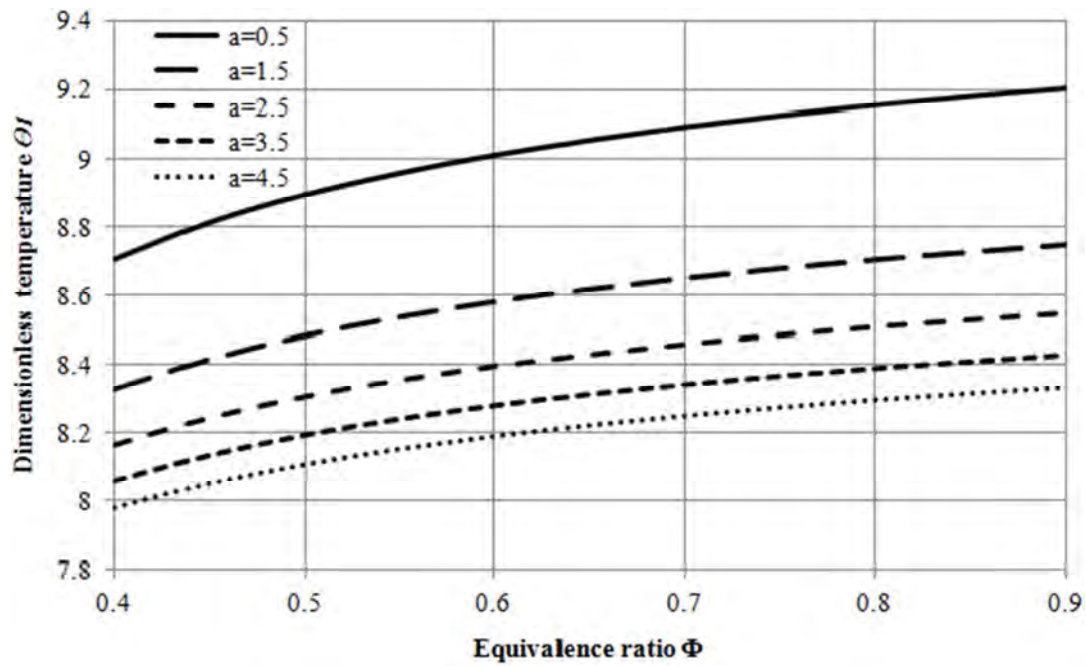
Figure 3. Dimensionless ultimate flame temperature as a function of equivalence ratio in different strain rates.

Figure 4 illustrates the comparison of this work's ultimate flame temperature with Huang et al. [13] in terms of equivalence ratio. As it is apparent, our flame temperature increases with a rise in the value of particle concentration. Similarly, the same trend can be seen in their study. It should be noted that the difference between the values of two flame temperatures is because of that the aluminum in [13] is liquid, while in our modeling aluminum has been used in solid phase and there is an energy loss due to conversion from solid to liquid phase. Therefore, solid particles burn at lower temperatures. In addition, Huang et al. [13] studied planar flame, while our modeling is based on counterflow configuration. However, we have a very low strain rate (a =0.5) here and it could be similar to the planar flame, but again the strain rate effect can be seen in Figure 4. This caused a decrease in the flame temperature in our modeling.
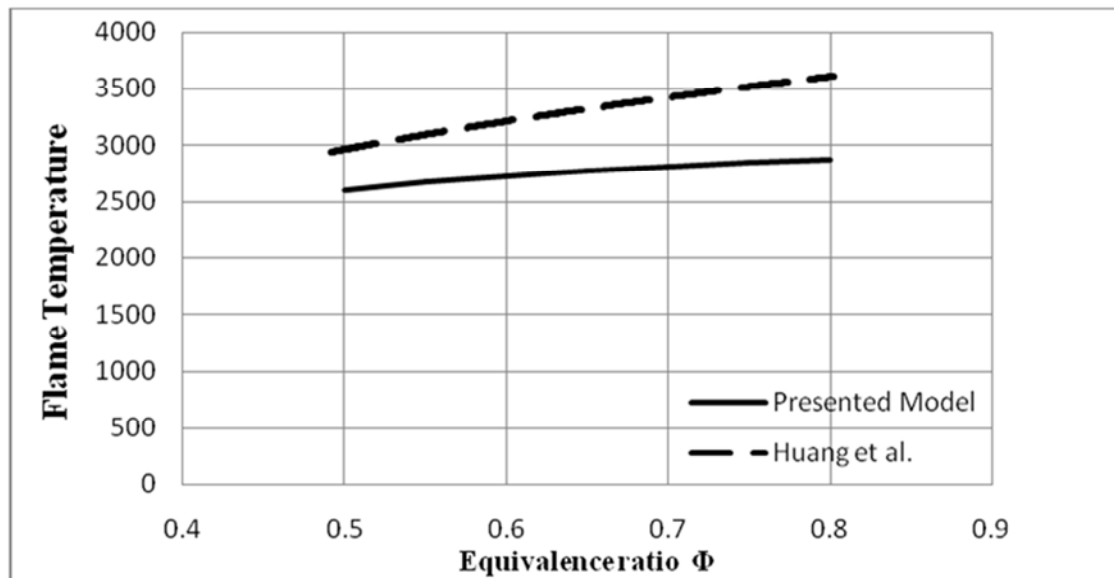

Figure 4. Flame temperature of aluminum-air mixture as function of equivalence ratio.

Figure 5 illustrates the dimensionless ignition temperature as a function of strain rate in different values of equivalence ratio. As it is apparent, temperature tends to decrease as strain rate rises. Also this figure elucidates that with a rise in the value of strain rate; the rate of change is going to slow down. So that, in the case of very low strain rates, the ignition temperature is higher.
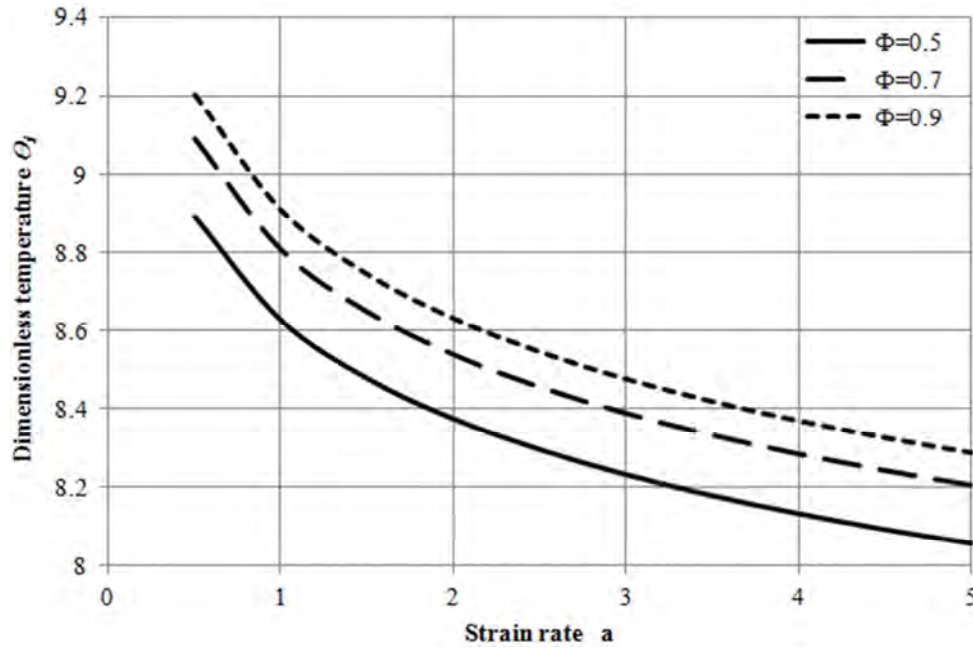
Figure 5. Dimensionless ignition temperature in terms of strain rate for different values of equivalence ratio.

Dimensionless place of ignition point in combustion of aluminum nano-particles as a function of equivalence ratio for different strain rates is demonstrated in Figure 6 with a rise in particle concentration the place of ignition point moves to the origin. When equivalence ratio rises, particle concentration increases at preheated zone, so it takes a longer time to reach their ignition temperature by heat conduction from the flame zone; and as a result, the place of ignition point moves to the origin. Also, one can conclude that in the case of high strain rates, after a certain value of particle concentration no significant change in the place of ignition point can be observed.
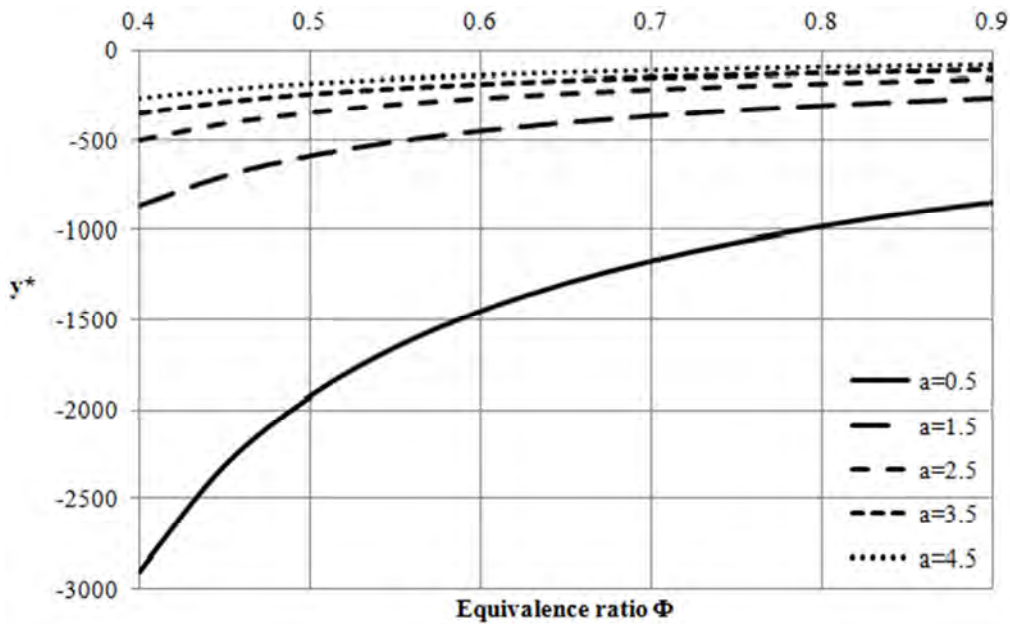

Figure 6. Dimensionless place of ignition point in terms of equivalence ratio for different values of strain rate.

Figure 7 illustrates the dimensionless place of ignition point in terms of strain rate for different values of equivalence ratio. As it is clear, the place of ignition point tends to move to the origin as the value of strain rate rises. But after a certain value of strain rate, the rate of change begins to slow down. So that, in the case of very low strain rates, the rate of change is much more than high strain rates.
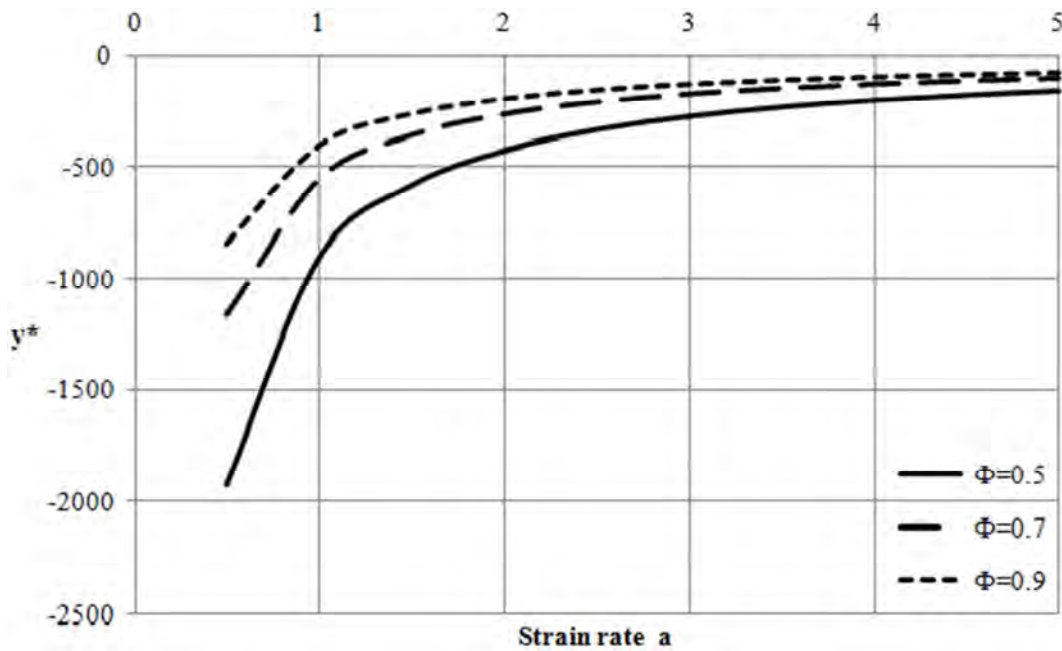
Figure 7. *Dimensionless place of ignition point as a function of strain rate in different equivalence ratio.*

Dimensionless flame thickness as a function of equivalence ratio in different strain rates is demonstrated in Figure 8. As it can be seen, with a rise in particle concentration the flame thickness decreases. It has reasonable agreement with Figure 7 where with a rise in particle concentration, the place of ignition point moves to the origin.
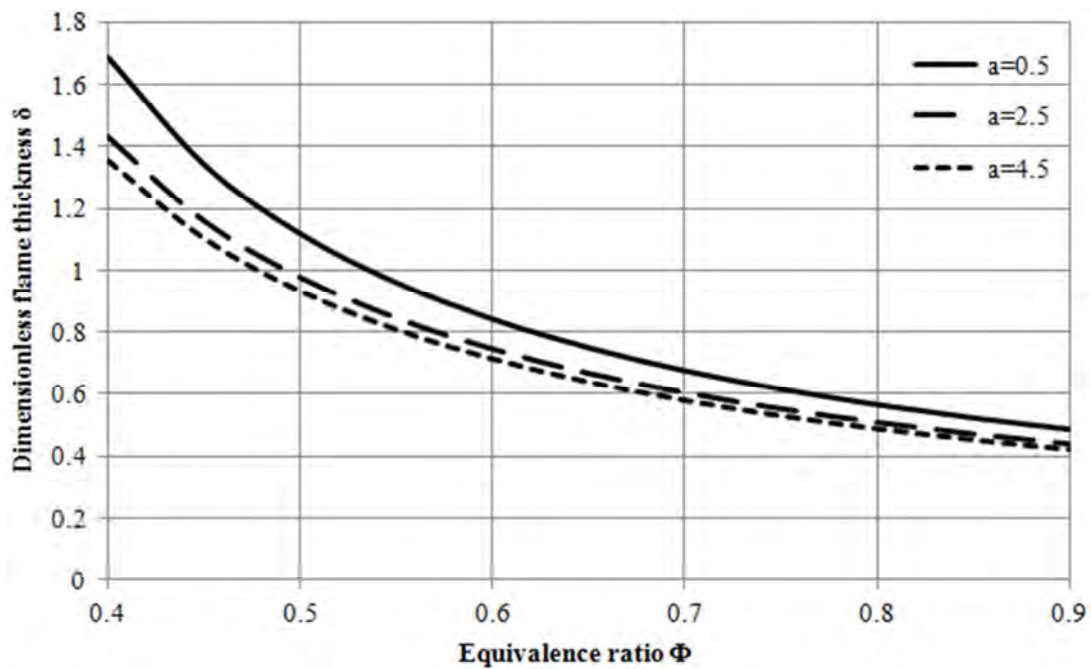

Figure 8. *Dimensionless flame thickness as a function of equivalence ratio in different strain rates.*

Figure 9 shows the dimensionless flame thickness in terms of strain rate for different values of equivalence ratio. As it is apparent, flame thickness tends to decrease as the strain rate rises. But as the strain rate rises, the rate of change begins to slow down and as it is clear, the value of flame thickness tends to have very small changes. Comparing Figure 8 and Figure 9 indicates that the equivalence ratio has more effects on the flame thickness than the strain rate.
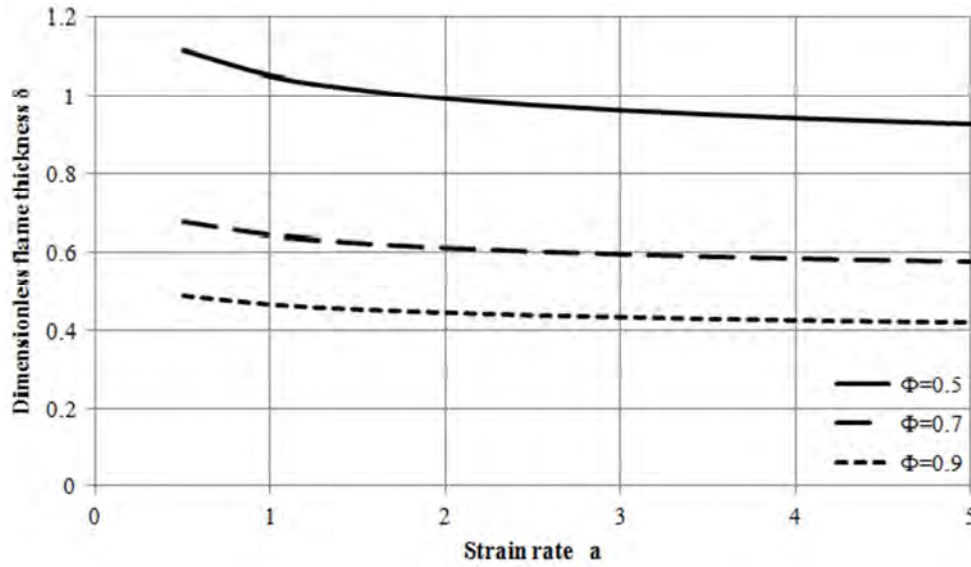
Figure 9. Dimensionless flame thickness as a function of strain rate in different equivalence ratio.

4. Conclusion

In this research, a mathematical model has been performed to analyze the structure of one dimensional premixed flame of aluminum nano-particles in a counterflow configuration. The flame has been assumed to consist of three zones: preheat, flame, and post flame regimes. According to the work of Goroshin et al. [12], burning time has been presumed, and the data has been obtained from experimental results. By non-dimensionalizing and solving the energy conservation equations for gas and particles, dimensionless temperatures of preheated and flame zones have been obtained, then diagrams of dimensionless ignition and ultimate flame temperatures, place of ignition point and flame thickness for different equivalence ratio and strain rate have been drawn.

The results indicate that with a rise in the value of particles concentration, the value of ignition and ultimate flame temperatures increase and the place of ignition point moves to origin so the flame thickness decreases. Furthermore, there is little difference between the values of ignition and ultimate flame temperature and it is because of very small flame thickness. Also, it is shown that as strain rate increases, the value of ignition temperature and flame thickness decreases and the place of ignition point move to origin. So that in the case of very low strain rates, the ignition temperature is higher and the rate of change in the place of ignition point is much more than high strain rates. Comparing the achieved results indicates that the equivalence ratio has more effects on the flame thickness than the strain rate. A reasonable agreement is observed between acquired results and previous work carried out by Huang et al. (Huang et al., 2005). It should be noted that these results are in the form of counterflow combustion and this study can lead to further research on the counterflow combustion of nano-particles.

Nomenclature

a	strain rate (s^{-1})
b	defined parameter, Eq. 21
C	specific heat capacity (kJ/kg.K)
D	particle diameter (cm)
E	activation energy (kJ/mol)
Q	heat of combustion (kJ/kg)
R	universal gas constant (kJ/K.kmol)
r	particle radius (m)
T	temperature (K)
υ	Gas velocity (m/s)
X_{eff}	Effective mole fraction of oxidizer
x	Defined parameter, Eq. 2
x'	Main coordinate, horizontal (m)
y	Dimensionless coordinate
y^*	Dimensionless place of ignition point
y_1	Dimensionless place of flame ending point
z'	Main coordinate, vertical (m)

Greek Symbols

γ	Dimensionless defined parameter
δ	Dimensionless flame thickness
ε	defined parameter, Eq. 18
θ	Dimensionless temperature
θ_1	Dimensionless flame ultimate temperature
κ	Dimensionless defined parameter
λ	Heat conduction coefficient (W/m.K)
μ	Dimensionless defined parameter
ρ	Density (kg/m^3)
σ	Concentration of particle (kg/m3)
τ_b	Burning time (s)
φ	Equivalence ratio
ω	Reaction rate (kg/m^3.s)

Superscript

*	starting point of flame zone

Subscripts

f	flame zone
u	entrance situation
s	solid aluminum particle
st	stoichiometric state
i	starting point of flame zone
si	ignition of solid particle

References

[1] Beckstead, M. (2004). A summary of aluminum combustion: DTIC Document.

[2] Beckstead, M. (2005). Correlating aluminum burning times. Combustion, Explosion and Shock Waves, 41(5), 533-546.

[3] Bidabadi, M., Mohammadi, M., Poorfar, A. K., Mollazadeh, S., & Zadsirjan, S. (2015). Modeling combustion of aluminum dust cloud in media with spatially discrete sources. Heat and Mass Transfer, 51(6), 837-845.

[4] Bidabadi, M., Mohammadi, M., Bidokhti, S. M., Poorfar, A. K., Zadsirjan, S., & Shariati, M. (2016). Modeling Flame Propagation of Coal Char Particles in Heterogeneous Media. Periodica Polytechnica. Chemical Engineering, 60(2), 85.

[5] Bidabadi, M., Ramezanpour, M., Mohammadi, M., & Fereidooni, J. (2016) The Effect of Thermophoresis on Flame Propagation in Nano-Aluminum and Water Mixtures. Periodica Polytechnica Chemical Engineering, Vol. 60, No. 3, pp. 157-164, 2016.

[6] Bocanegra, P. E., Chauveau, C., & Gökalp, I. (2007). Experimental studies on the burning of coated and uncoated micro and nano-sized aluminium particles. Aerospace science and technology, 11(1), 33-38.

[7] Brooks, K. P., & Beckstead, M. W. (1995). Dynamics of aluminum combustion. Journal of Propulsion and Power, 11(4), 769-780.

[8] Chen, Z., & Fan, B. (2005). Flame propagation through aluminum particle cloud in a combustion tube. Journal of loss prevention in the process industries, 18(1), 13-19.

[9] Daou, J. (2011). Strained premixed flames: Effect of heat-loss, preferential diffusion and reversibility of the reaction. Combustion Theory and Modelling, 15(4), 437-454.

[10] Dreizin, E. L. (1996). Experimental study of stages in aluminium particle combustion in air. Combustion and Flame, 105(4), 541-556.

[11] Dreizin, E. L., & Trunov, M. A. (1995). Surface phenomena in aluminum combustion. Combustion and Flame, 101(3), 378-382.

[12] Goroshin, S., Kolbe, M., & Lee, J. H. (2000). Flame speed in a binary suspension of solid fuel particles. Proceedings of the Combustion Institute, 28(2), 2811-2817.

[13] Huang, Y., Risha, G. A., Yang, V., & Yetter, R. A. (2005). Analysis of nano-aluminum particle dust cloud combustion in different oxidizer environments. Paper presented at the 43rd AIAA Aerospace Sciences Meeting and Exhibit, Reno, NV.

[14] Huang, Y., Risha, G. A., Yang, V., & Yetter, R. A. (2007). Combustion of bimodal nano/micron-sized aluminum particle dust in air. Proceedings of the Combustion Institute, 31(2), 2001-2009.

[15] Huang, Y., Risha, G. A., Yang, V., & Yetter, R. A. (2009). Effect of particle size on combustion of aluminum particle dust in air. Combustion and Flame, 156(1), 5-13.

[16] Il'in, A., Gromov, A., Vereshchagin, V., Popenko, E., Surgin, V., & Lehn, H. (2001). Combustion of ultrafine aluminum in air. Combustion, Explosion and Shock Waves, 37(6), 664-668.

[17] Ivanov, G. V., & Tepper, F. (1997). 'Activated'Aluminum as a Stored Energy Source for Propellants. International Journal of Energetic Materials and Chemical Propulsion, 4(1-6).

[18] Kwon, Y.-S., Gromov, A. A., Ilyin, A. P., Popenko, E. M., & Rim, G.-H. (2003). The mechanism of combustion of superfine aluminum powders. Combustion and Flame, 133(4), 385-391.

[19] Liu, F., Daun, K., Snelling, D. R., & Smallwood, G. J. (2006). Heat conduction from a spherical nano-particle: status of modeling heat conduction in laser-induced incandescence. Applied physics B, 83(3), 355-382.

[20] Mohammadi, M., Bidabadi, M., Khalili, H., & Poorfar, A. K. (2016). Modeling Counterflow Combustion of Dust Particle Cloud in Heterogeneous Media. Journal of Energy Engineering, 04016040.

[21] Nayfeh, A. H. (2011). Introduction to perturbation techniques: John Wiley & Sons.

[22] Rand, R. H., & Armbruster, D. (1988). Perturbation methods, bifurcation theory and computer algebra: Springer-Verlag New York, Inc.

[23] Risha, G. A., Huang, Y., Yetter, R. A., & Yang, V. (2005). Experimental investigation of aluminum particle dust cloud combustion. Paper presented at the 43 rd Aerospace Sciences Meeting and Exhibit, AIAA.

[24] Shoshin, Y. L., & Dreizin, E. L. (2006). Particle combustion rates for mechanically alloyed Al–Ti and aluminum powders burning in air. Combustion and Flame, 145(4), 714-722.

[25] Sun, J., Dobashi, R., & Hirano, T. (2006). Structure of flames propagating through aluminum particles cloud and combustion process of particles. Journal of loss prevention in the process industries, 19(6), 769-773.

[26] Thatcher, R., & Al Sarairah, E. (2007). Steady and unsteady flame propagation in a premixed counterflow. Combustion Theory and Modelling, 11(4), 569-583.

[27] Wang, H., Chen, W., & Law, C. (2007). Extinction of counterflow diffusion flames with radiative heat loss and nonunity Lewis numbers. Combustion and Flame, 148(3), 100-116.

[28] Yetter, R. A., & Dryer, F. L. (2001). Metal Particle Combustion and Classification, Micro-gravity Combustion: Fire in Free Fall: Academic Press.